Dynamic, Robust Locomotion for a Non-Anthropomorphic Biped

Min Sung Ahn[1] and Dennis Hong[1]

***Abstract*— This work presents a dynamic walking controller for a high-bandwidth torque-controlled non-anthropomorphic bipedal robot. A simplified model with passive stability characteristics is leveraged along with feedback linearization techniques, actively adjusted footstep positions, and swing leg trajectories that minimize the creation of additional moments, to make the robot follow a desired velocity under different environmental circumstances. Tests to show the approach's robustness to external forces and imperfect terrain (e.g. stairs, obstacles, ramps) are demonstrated in simulation. Dynamic stability of the approach is analyzed through a limit cycle analysis.**

I. INTRODUCTION

Legged robots have a unique advantage against its rolling wheeled counterparts as discrete footstep positions can be reached to traverse non-continuous and unstructured terrain, forces can be applied to its surrounding environment, and the center of mass (COM) position can be moved without moving its foothold. This is especially advantageous in outdoor and man-made environments where sporadically dispersed obstacles or terrains with different levels of elevation such as stairs and roadblocks are common. To stably traverse these habitats, more recently quadrupeds and hexapods have been actively developed. ANYbotic's ANYmal platform successfully demonstrated an ability to inspect an oil rig site, which consisted of various stairs and elevated platforms [1]. Boston Dynamic's Spot is commercially available for select customers to rigorously test at construction sites and for surveillance purposes. ALPHRED is also fully capable of picking up and putting down a package to successfully conduct the last-mile delivery problem for robotics [2]. On a more extreme case, an optimal COM positioning combined with a force profile on vertical walls can be applied by a hexapod to demonstrate extreme mobility such as climbing walls [3]. However, despite the impressive performance of quadrupeds and hexapods, one downside is the amount of ground real estate they occupy, which can be scarce in narrow corridors.

In this sense, bipedal platforms have an advantage over its counterparts with more legs because the amount of space they require is significantly less. However, bipedal platforms, as exposed in the DARPA Robotics Challenge, is inherently an unstable platform where the stability is exacerbated by the moment created by its forward swinging legs. While complex control approaches could be used to make the platform maintain its balance and walk, to fundamentally approach the bipedal walking problem from a design perspective, NABi-1 was created [4].

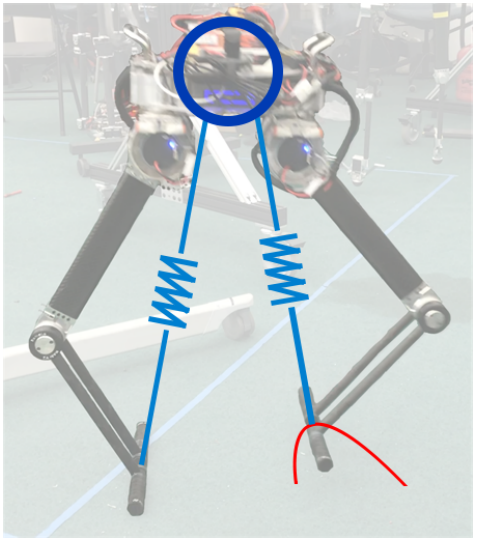

Fig. 1. The walking controller tries to guide the robot based on a dual spring-loaded inverted pendulum. The red trajectory is an example Bezier curve that the swing leg follows.

The idea behind the NABi lineage of robots is that by constraining the robot's movement into a plane, complexity stemming from the moment created by the swing leg of a traditionally forward walking bipedal robot is eliminated. Consequently, a simple change in the mechanical design greatly simplifies the controls. However, studies in biomechanics do show that sideways walking can be inefficient [5]. With NABi-1, because it had springs at its feet to both stabilize itself and store energy which can be used to dynamically propel itself forward, the robot could efficiently and stably walk [4]. However, being able to only walk in a 2D plane because of the lack of joints is a major disadvantage. Therefore, NABi-2 was built with the addition of an extra joint per leg.

NABi-2 is a torque-controlled bipedal platform with three degrees of freedom per leg using proprioceptive actuators [6]. To prevent falling over without any ankle actuation, NABi-2 is equipped with bar feet such that when its legs are sufficiently spread apart, the convex hull generated by its feet is some form of a quadrilateral. Then, as is well known in literature [7], positioning its vertical projection of its center of mass inside the convex hull can prevent a fall. However, because NABi-2 does not have such energy storage and because of the reduced stability provided by the lack of

*This work was supported by the ONR through grant N00014-15-1-2064.

[1]All authors are with the Robotics and Mechanisms Laboratory (RoMeLa) at the University of California, Los Angeles (UCLA), Los Angeles, CA 90095, USA. The corresponding author can be reached at aminsung@ucla.edu.

springs, so far its main form of locomotion has been pronking [8] and virtual constraint-based quasi-static walking [9].

Pronking can be a solution for locomotion, but the reduced ground contact time gives less balance opportunities for the robot, making it vulnerable to unexpected disturbances. The assumptions made in the approach taken for NABi-1 is less true with NABi-2 (i.e. existence and lack of a support polygon at all times), which reduced the approach's applicability on the new platform. The quasi-static approach can make NABi-2 walk, but is not dynamically stable, making it susceptible to disturbances and imperfections on the ground. In this sense, this work proposes a new locomotion controller that is more dynamic and robust for a bipedal robot such as NABi-2. Particularly, similar to how NABi-1 took advantage of its mechanical hardware (e.g. springs), this work attempts to exploit the high bandwidth of the proprioceptive actuators to achieve stable locomotion indirectly present in the simplified model for the task of walking in unstructured terrain and following a commanded velocity.

The main contribution of this work is in two folds:

- Leverage an inherently stable, simplified model to achieve dynamic yet stable locomotion using high bandwidth torque inputs.
- Demonstrate the robustness of the controller in a wide variety of unstructured environments at a commanded velocity.

This work is organized in the following order. Section II introduces existing bipedal locomotion strategies while Section III explains this work's approach. Section IV presents and discusses the results of the controller tested on various environments. Finally, Section V concludes the work as well as introducing potential future work.

II. BACKGROUND

There have been many attempts to find stable yet natural locomotion approaches for bipedal robots. Depending on the platform that is being used, different approaches have seen success, despite the fundamental differences between them. However, they can primarily be categorized into statically stable methods and dynamically stable methods.

Statically stable methods, where the robot never falls even if it froze, revolve around the idea of maintaining the ground projected center of mass within the convex hull (support polygon) made by the points of contact with the ground. There are seminal works that use the concept of the Zero Moment Point (ZMP) [10] with a preview controller to guide a humanoid to step at a sequence of pre-defined footstep positions which happens to maintain the ZMP within the convex hull [11]. Similar ideas using the ZMP except within an optimization framework have also been explored [12]. Historically, fully actuated bipeds have seen great success within this framework [13] [14] [15] [16].

Dynamically stable methods may result in the robot falling if it freezes. Unlike the statically stable methods which are often associated with slower motions, approaches that pursue dynamic stability can allow a robot to conduct lively motions such as balancing, faster walking, and even running. These methods often allow the gravitational force and the natural dynamics of the system to play a role in the motion. At an extremity, there exists passive walkers that walk with zero actuation [17], which also led to the development of hybrid zero dynamics approaches [18] [19]. These robots are underactuated with point feet, which makes analyzing stability with the ZMP framework inappropriate.

Biology has also been an inspiration in control as natural dynamics began to be leveraged. Simplified models such as the spring-loaded inverted pendulum (SLIP)—a dynamic model that better represents animal locomotion—led to development of robots [20] and controllers [21] [22] that demonstrated dynamic locomotion while still being energetically efficient, as the natural dynamics could alleviate the work from the actuators.

This work shares the flavor of utilizing the natural dynamics of the robot for an underactuated biped, using a simplified model that naturally tries to converge to a stable limit cycle [23]. However, rather than making the controller for a robot with fixed dynamics (i.e. unchangeable springs), this work guides the robot to behave like it has a certain dynamics by leveraging its high-bandwidth torque-controlled backdrivable actuators [6] and imposing motions that are output by the pre-propagated dynamics. Assuming the dynamics are imposed, the robot would be able to converge to a stable limit cycle in presence of disturbances.

III. FORMULATION & CONTROL

Similar to [9], this work assumes NABi-2 as a planar platform, ignoring the yaw authority in both legs which allow NABi-2 to extend its legs out of a plane. Therefore, the generalized coordinates are $q = [x, z, \phi]$, where x and z are the horizontal and vertical positions of the center of mass, and ϕ is the body pitch angle relative to the inertial frame. Note that variables with respect to the body frame are denoted by a preceding $\mathcal{B}$ superscript while those without it are relative to the inertial frame.

The mathematical model used to represent NABi-2's dynamics assumes a point mass at the robot's center of mass, massless legs, and a point contact with the ground. Such simplified models are widely used in both biomechanics and legged robotics because they are easy to analyze and especially with robots, the dynamics of the leg can be removed from acting as a disturbance. In this sense, the model used to represent NABi-2 is a dual spring-loaded inverted pendulum model as seen in Fig. 1. Each SLIP represents each of the robot's legs. This model also has an attractive advantage where if a time-based input trajectory with a phase difference is given, it can return to its original cycle from any initial condition, which makes the locomotion strategy robust from the mathematical modeling stage. Consequently, locomotion on imperfect terrain would be achievable. Assuming this model, a separate stance leg and swing leg control are executed, with the former attempting to apply the pre-computed ground reaction force profile to keep

the body afloat while the latter controls the actual locomotion speed.

A. Stance Leg Control

While many bipedal locomotion strategies use a combination of single support (one leg in contact with the ground) and double support (two legs in contact with the ground), this work does not explicitly dedicate a time interval for double support. In fact, each leg takes turns applying a force profile to the ground while the other leg simply swings. The ground reaction force profile is generated based on the aforementioned dual SLIP model. Such a model has two inputs ($f_{m,1}, f_{m,2}$) in a 1-D case as seen in Eqn. 1, where the inputs are offset with a pre-defined phase.

$$m\ddot{z} = f_{m,1} + f_{m,2} - mg \tag{1}$$

where $f_{m,i}, i = 1, 2$ is defined as:

$$f_{m,i} = \begin{cases} k_{p,\mathrm{t}}(d - z) + k_{d,\mathrm{t}}(\dot{d} - \dot{z}), & \text{if } d > z. \\ 0, & \text{otherwise.} \end{cases} \tag{2}$$

and $k_{p,\mathrm{t}}$, $k_{d,\mathrm{t}}$ are intuitively the spring and damper constants and d is a sinusoidal signal set to inject a non-negative input if the body height drops below d.

When the swing leg impacts the ground, the above dynamics are propagated for one step time interval with the current body height z and body height velocity $\dot{z}$ using the Runge-Kutta method [24], which outputs both $f_{m,1}$ and $f_{m,2}$. The input corresponding to the new stance leg (i.e. the swing leg that just impacted the ground) is set as F_z, where F is the desired ground reaction force in the Z direction in the inertial frame.

The robot is also susceptible to tilting in the direction of the swing leg when the swing leg is lifted from the ground because the support polygon that the center of mass should be in disappears as all contact with the ground are point contacts in the planar case. If not accounted for, this can directly affect the position of the swing leg's foot at the time of impact, which affects the ability to track a desired center of mass velocity. This issue could be alleviated if the deviation of ϕ from 0 is minimized. Consequently, a feedback linearization control input is formulated where given the equation of motion using the Euler-Lagrange equation:

$$M(q)\ddot{q} + C(q, \dot{q})\dot{q} + g(q) = Bu \tag{3}$$

where $M(q)$ is the inertia matrix, $C(q, \dot{q})$ is the Centrifugal-Coriolis matrix, $g(q)$ is the gravity vector, and B is the appropriate mapping matrix, the following control input is generated:

$$u = \frac{-L_f^2\phi + w}{L_f L_g \phi} \tag{4}$$

$$w = -k_p(\phi - \phi_d) - k_d(\dot{\phi} - \dot{\phi}_d) \tag{5}$$

where $L_f\phi$ is the Lie derivative of ϕ with respect to f, where f and g are the affine representation of Eqn. 3:

$$f = \begin{bmatrix} \dot{q} & M(q)^{-1}(-C(q, \dot{q})\dot{q} - g(q)) \end{bmatrix}^\top \tag{6}$$

$$g = \begin{bmatrix} 0 & M(q)^{-1}B \end{bmatrix}^\top \tag{7}$$

and ϕ_d is the desired pitch angle of the robot. The computed u then becomes the desired F_x.

B. Swing Leg Control

While the stance leg is applying the computed ground reaction force profile to keep the body afloat following the dual SLIP dynamics and body pitch oriented close to 0, the swing leg reaches towards a desired footstep position and consequently affects the actual linear velocity of the robot. To reach the desired position at touchdown, a combination of a constantly updated swing leg trajectory based on the body's orientation, operational space control of the foot, as well as an early touchdown detection based on a disturbance observer [25] is used.

To begin with, the desired footstep position is responsible for determining the velocity that the robot will travel at. It uses a combination of Raibert heuristics [26] as well as Capture Point dynamics [27] at a pre-defined nominal offset relative to the COM, as seen in Eqn. 8:

$$p_{fs,d} = Rp_{fs,n} + \frac{\dot{p}_{com}T_s}{2} + W_{cp}\sqrt{\frac{z}{g}}(\dot{p}_{com} - \dot{p}_{com,d}) \tag{8}$$

where p is the position of the footstep (fs) and COM (com), R is the orientation of the body, and W_{cp} is a gain to determine the effect the Capture Point dynamics has in the determination of the footstep.

Provided the footstep position, a swing leg trajectory that is favorable for the NABi configuration is generated online. As aforementioned, because of the rod feet that is a point in the planar case, NABi-2 is prone to falling over when there are greater amount of extended mass away from its pivot point. Therefore, to reach the desired footstep positions, a Bezier curve that promotes lifting the foot close to the body and quickly extending to the desired position is designed. Consequently, depending on the walking direction, three control points are computed online, which the Bezier curve is built on. A sample trajectory is shown in Fig. 1. This trajectory is tracked using an operational space formulation:

$$\begin{aligned} {}^{\mathcal{B}}f_{sw} = J^T(q)\Lambda(q)[k_{p,\mathrm{sw}}(R^T p_{fs,d} - {}^{\mathcal{B}}p_{fs}) \\ - k_{d,\mathrm{sw}}{}^{\mathcal{B}}\dot{p}_{fs}] \end{aligned} \tag{9}$$

where J is the Jacobian, Λ is the operational space inertia matrix, and $k_{p,\mathrm{sw}}$ and $k_{d,\mathrm{sw}}$ are the position and velocity gains. Note that the desired profile in the inertial frame is rotated to the body frame to account for the constant change in the body pitch.

IV. RESULTS & DISCUSSION

This section presents the results from various tests that the controller was assessed on. Because this work focuses on a new controller that would enhance the current performance of NABi-2 in terms of robustness to disturbance and imperfect terrain through dynamic walking, after initially demonstrating the capability to track a commanded

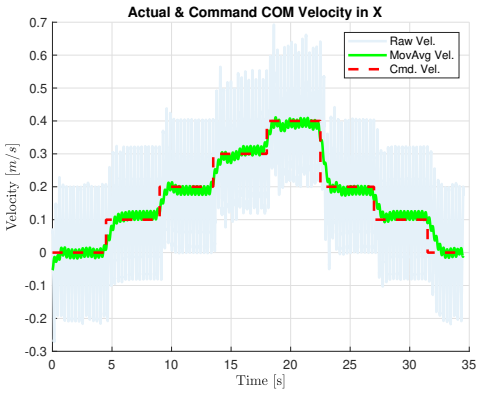

Fig. 2. The commanded velocity overlayed on the actual velocity. Because the raw velocity signal is noisy, a moving average value based on a sliding window of 500 is also shown.

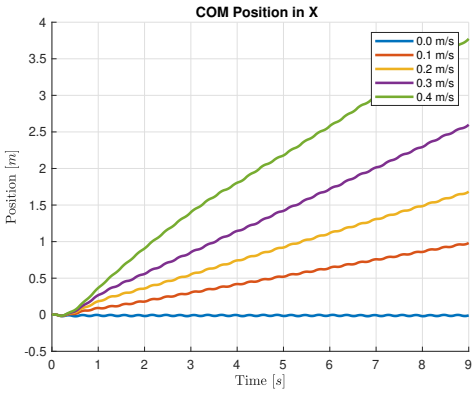

Fig. 3. Actual position of the COM at a given time for different commanded velocities. It is noticeable that as the velocity of the robot increases, periods where the robot comes to a stop (slope of 0) decreases.

velocity on flat ground, the ability to overcome unexpected periods of disturbances are assessed afterwards. Following, to demonstrate robustness to an environment with non-flat and discontinuous terrains, the controller is tested to guide the robot to walk over stairs and unknown blocks without perception data. As a generalization of the terrain test, the robot is commanded to ascend and descend an asymmetrical slope. Finally, the dynamic stability of the robot is analyzed.

The environment is built using CoppeliaSim [28] with Bullet [29] as the backend physics engine. All control is simulated at 500 Hz and the communication between the controller and the simulated robot is non-blocking. The full specifications of the robot are as in [8].

A. Tracking Velocity Profile on Flat Ground

As aforementioned, tracking a COM velocity profile is done through footstep placement. After initialization, the robot is commanded by the operator to walk at a given velocity. As see in Fig. 2, the robot is commanded to initially walk in place, and then step inputs to higher velocities by increments of $0.1m/s$ are commanded up to $0.4m/s$ at $4.5s$ spells until it is ramped back down to zero at intervals of $0.2m/s$ and $0.1m/s$. With a smoother increase in commanded velocity, the controller could successfully command the robot up until $0.6m/s$. While the moving average velocity is close to the desired velocity, the unfiltered, raw velocity of the robot is quite noisy, as it oscillates around the desired velocity at every step.

Fig. 3 also shows the position of the output by the state estimation. NABi-2 shows an oscillatory behavior when walking. An interesting phenomena is that as the linear velocity decreases, the amount of time that the slope of the curve is at zero increases. This is in line with previous studies that observed repeated stops (slope of zero) when walking sideways.

B. Disturbance Rejection

To gauge how robust the robot is to external impacts, disturbance during walking is applied in the walking direction and against the walking direction at various times as opposed to at a specific time during the walking cycle. Also, rather than an instantaneous disturbance, it is continuously applied for $100ms$.

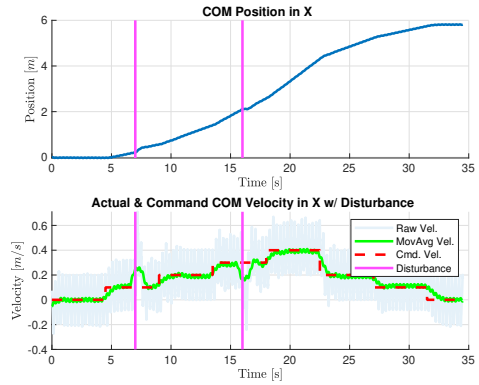

Fig. 4. Top: COM position during the duration of the test. The robot's position rapidly increases when pushed forward, while it becomes stationary when pushed against the walking direction. Bottom: Velocity of the robot, where the external disturbance of $20Nm$ in the walking direction at $7s$ and against the walking direction at $16s$ can be observed. The robot is able to recover and follow the commanded velocity within the following $2s$.

Fig. 4 (bottom) shows the commanded velocity and the actual velocity of the robot while Fig. 4 (top) shows the robot's position as measured by the estimator. The graph clearly shows times when the robot is pushed towards and against its walking direction. However, as the desired footstep positions are actively updated, the robot is able to recover. Furthermore, because all the NABi-series robots have a unique configuration where the robot's knee joint is protruded outwards, in reality, a frequent point of collision or disturbance is also at the knee. Consequently, non-instantaneous disturbance was also applied at the knee against the walking direction for the front leg and towards it for the back leg. Similarly, the controller was able to stabilize the robot.

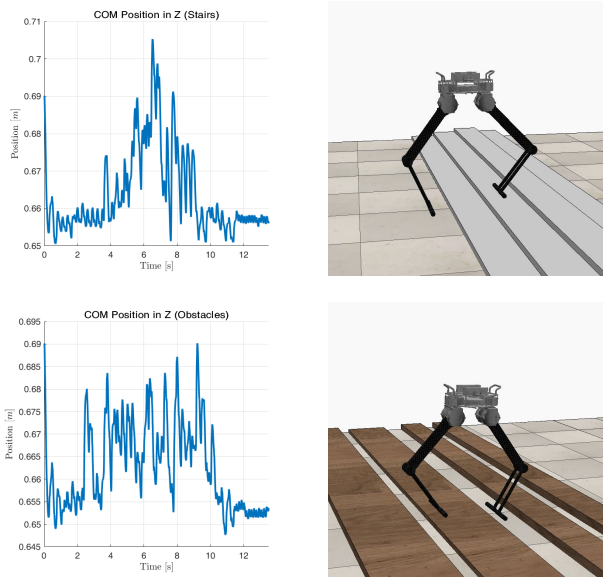

Fig. 6. Top-Left: Body height while walking up and down the stairs. Top-Right: NABi-2 walking across stairs. Bottom-Left: Body height while walking across a terrain with randomly positioned blocks. Bottom-Right: NABi-2 walking across randomly positioned obstacles.

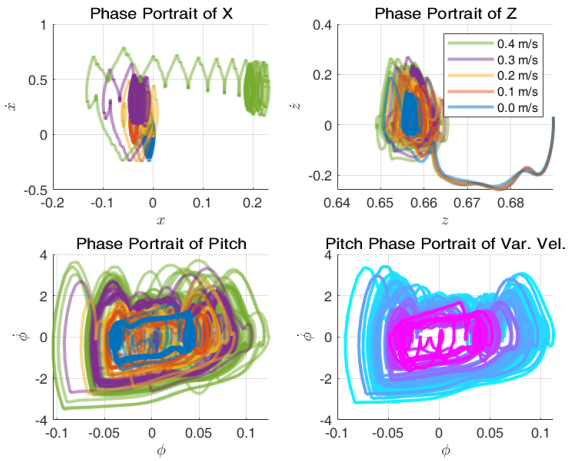

Fig. 7. Top-Left: Phase portrait of x and $\dot{x}$. Top-Right: Phase portrait of z and $\dot{z}$. Bottom-Left: Phase portrait of ϕ and $\dot{\phi}$. Bottom-Right: Evolution of the phase portrait of ϕ and $\dot{\phi}$ as the actual velocity increases from $0.0m/s$ (magenta) to $0.4m/s$ (cyan) at increments of $0.1m/s$.

C. Perception-less Locomotion on Non-Flat and Non-Continuous Terrain

To demonstrate the robustness of the controller to non-flat terrain, the controller is tested on a ground with stairs and randomly positioned blocks. Considering the size of the robot, steps as high as $6cm$ per step and blocks that are up to $10cm$ tall are randomly spaced out.

Fig. 6 (top-left) shows the COM height when ascending and descending the stairs and Fig. 6 (bottom-left) shows the height when walking with randomly positioned blocks. In both cases, when the robot detects an unexpected change in height, it ascends/descends accordingly as the time-based force trajectory naturally maintains a certain distance between the feet and the body. Additionally, because the time-based force trajectory results in a double-hump COM trajectory in an ideal situation, this behavior continues to be present despite the rapid change in the height of the ground.

As a generalization of the change in the height of the ground, rather than on an environment with flat surfaces, the controller is tested on one with a curved surface (i.e. ramp) as seen in Fig. 5. The robot was commanded at a lower velocity than when tested on the stairs because it would often slip while descending. Regardless, at a slower velocity ($0.2m/s$ in the case shown), the robot was able to successfully ascend and descend a curved surface.

D. Dynamic Stability

To go beyond simply determining the success of the controller and its robustness to unknown terrain and disturbances by its physical behavior, the dynamic stability of the robot is gauged by observing the phase portraits of the generalized coordinates and conducting a limit cycle analysis. Fig. 7 presents the phase portraits, where Fig. 7 (top-left), (top-right), and (bottom-left) are data from when the robot was immediately commanded from $0.0m/s$ to the velocities shown in the legend. All graphs show convergence to a limit cycle, albeit a difference in transient time as seen in Fig. 7 (top-left). Additionally, while a formal Poincaré analysis is not possible, Fig. 8 shows the phase portraits for a pair of steps (one step each for front and back legs), which clearly shows the existence of a cycle and confirms the dynamic stability of the robot.

What is also especially interesting is how the phase portraits of z and ϕ generally expand as the velocity increases. Fig. 7 (bottom-right) shows the phase portrait of ϕ for the run shown in Fig. 2 up until the beginning of the slowdown. It is clear that in the midst of what seems to be chaotic behavior during a change in velocity, the controller still guides the robot to converge to its limit cycle.

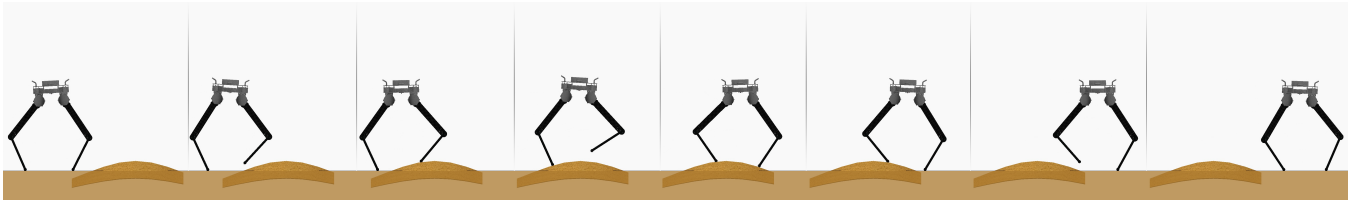

Fig. 5. Snapshots of the controller guiding NABi-2 over a ramp without any perception data.

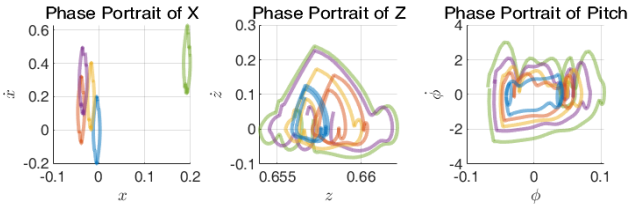

Fig. 8. The generalized coordinate's phase portrait for a single step cycle where one step is taken for each of the front and back legs. The legends are the same as Fig. 7.

V. CONCLUSION & FUTURE WORK

This work focuses on the details of a robust walking controller for a non-anthropomorphic bipedal robot in a planar setting. By leveraging the high-bandwidth backdrivable properties of the robot's actuators, a desired dynamics that converges to a stable limit cycle when provided a time-based input trajectory is executed on the robot. Feedback linearization and actively updated desired footstep trajectories based on a Bezier curve that reduces instability due to extended leg inertia collectively assist with the execution of a desired ground reaction force profile. The feasibility of the approach and its dynamic stability was validated through a series of simulations where the robot was controlled to follow a sequence of command velocities despite disturbance applied at the center of mass, and without perception data, walk over imperfect terrains consisting of stairs, randomly placed obstacles, and a curved ramp. By observing the phase portraits of the generalized coordinates, a convergence to a limit cycle is noticeable and the qualitative shape of the cycle simply expands as the velocity is increased.

Going forward, the controller will also be tested and verified on the actual hardware to see how well the desired dynamics can be executed. While the simulation tried to replicate the behavior of NABi-2's unique actuators and its inertial properties, it only validates the controller's feasibility but does not guarantee that the chosen force profiles will work.

In this sense, there clearly is additional work that will be investigated as the controller is evaluated on the physical platform. The inevitable inaccuracies in the simulation model and the hardware opens up opportunities for finding the right dynamics to ask NABi to replicate. While this could be through repeated experiments of finding the $k_{p,\mathrm{t}}$ and $k_{d,\mathrm{t}}$ values, an autonomous agent could also be trained in a reinforcement learning (RL) framework to find these values. This also allows tackling an important aspect of the original SLIP-embedded methods—energetic efficiency. Trying to find the best dynamics for NABi-2 to execute while being both stable and energetically efficient is a non-intuitive task. However, within an optimization or RL framework, efficiency can explicitly be included in the cost/reward and be minimized while feasible dynamics are also found. Further down, comparison to purely end-to-end RL-based approaches or purely optimization approaches (e.g. model predictive control) and looking for the right balance between utilizing the natural dynamics of the actual system and enforcing a certain dynamical behavior through high-bandwidth backdrivable actuators will also be looked at.

REFERENCES

[1] M. Hutter, C. Gehring, A. Lauber, F. Gunther, C. D. Bellicoso, V. Tsounis, P. Fankhauser, R. Diethelm, S. Bachmann, M. Blösch *et al.*, "Anymal-toward legged robots for harsh environments," *Advanced Robotics*, vol. 31, no. 17, pp. 918–931, 2017.

[2] J. Hooks, M. S. Ahn, J. Yu, X. Zhang, T. Zhu, H. Chae, and D. Hong, "Alphred: A multi-modal operations quadruped robot for package delivery applications."

[3] X. Lin, J. Zhang, J. Shen, G. Fernandez, and D. W. Hong, "Optimization based motion planning for multi-limbed vertical climbing robots," *arXiv preprint arXiv:1909.06339*, 2019.

[4] J. Yu, J. Hooks, S. Ghassemi, A. Pogue, and D. Hong, "Investigation of a non-anthropomorphic bipedal robot with stability, agility, and simplicity," in *2016 13th International Conference on Ubiquitous Robots and Ambient Intelligence (URAI)*. IEEE, 2016, pp. 11–15.

[5] M. L. Handford and M. Srinivasan, "Sideways walking: preferred is slow, slow is optimal, and optimal is expensive," *Biology letters*, vol. 10, no. 1, p. 20131006, 2014.

[6] T. Zhu, J. Hooks, and D. Hong, "Design, modeling, and analysis of a liquid cooled proprioceptive actuator for legged robots," in *2019 IEEE/ASME International Conference on Advanced Intelligent Mechatronics (AIM)*. IEEE, 2019, pp. 36–43.

[7] P.-B. Wieber, "On the stability of walking systems," 2002.

[8] J. Yu, J. Hooks, X. Zhang, M. S. Ahn, and D. Hong, "A proprioceptive, force-controlled, non-anthropomorphic biped for dynamic locomotion," in *2018 IEEE-RAS 18th International Conference on Humanoid Robots (Humanoids)*. IEEE, 2018, pp. 1–9.

[9] J. Yu, "Control implementation of dynamic locomotion on compliant, underactuated, force-controlled legged robots with non-anthropomorphic design," 2020.

[10] M. Vukobratović and B. Borovac, "Zero-moment point—thirty five years of its life," *International journal of humanoid robotics*, vol. 1, no. 01, pp. 157–173, 2004.

[11] S. Kajita, F. Kanehiro, K. Kaneko, K. Fujiwara, K. Harada, K. Yokoi, and H. Hirukawa, "Biped walking pattern generation by using preview control of zero-moment point," in *2003 IEEE International Conference on Robotics and Automation (Cat. No. 03CH37422)*, vol. 2. IEEE, 2003, pp. 1620–1626.

[12] L. Saab, O. E. Ramos, F. Keith, N. Mansard, P. Soueres, and J.-Y. Fourquet, "Dynamic whole-body motion generation under rigid contacts and other unilateral constraints," *IEEE Transactions on Robotics*, vol. 29, no. 2, pp. 346–362, 2013.

[13] K. Kaneko, F. Kanehiro, M. Morisawa, K. Akachi, G. Miyamori, A. Hayashi, and N. Kanehira, "Humanoid robot hrp-4-humanoid robotics platform with lightweight and slim body," in *2011 IEEE/RSJ International Conference on Intelligent Robots and Systems*. IEEE, 2011, pp. 4400–4407.

[14] H. Wang, Y. F. Zheng, Y. Jun, and P. Oh, "Drc-hubo walking on rough terrains," in *2014 IEEE International Conference on Technologies for Practical Robot Applications (TePRA)*. IEEE, 2014, pp. 1–6.

[15] S. G. McGill, S.-J. Yi, H. Yi, M. S. Ahn, S. Cho, K. Liu, D. Sun, B. Lee, H. Jeong, J. Huh *et al.*, "Team thor's entry in the darpa robotics challenge finals 2015," *Journal of Field Robotics*, vol. 34, no. 4, pp. 775–801, 2017.

[16] S.-J. Yi, S. McGill, H. Jeong, J. Huh, M. Missura, H. Yi, M. S. Ahn, S. Cho, K. Liu, D. Hong *et al.*, "Robocup 2015 humanoid adultsize league winner," in *Robot Soccer World Cup*. Springer, 2015, pp. 132–143.

[17] T. McGeer *et al.*, "Passive dynamic walking," *I. J. Robotic Res.*, vol. 9, no. 2, pp. 62–82, 1990.

[18] J. W. Grizzle, G. Abba, and F. Plestan, "Asymptotically stable walking for biped robots: Analysis via systems with impulse effects," *IEEE Transactions on automatic control*, vol. 46, no. 1, pp. 51–64, 2001.

[19] E. R. Westervelt, J. W. Grizzle, and D. E. Koditschek, "Hybrid zero dynamics of planar biped walkers," *IEEE transactions on automatic control*, vol. 48, no. 1, pp. 42–56, 2003.

[20] C. Hubicki, J. Grimes, M. Jones, D. Renjewski, A. Spröwitz, A. Abate, and J. Hurst, "Atrias: Design and validation of a tether-free 3d-capable spring-mass bipedal robot," *The International Journal of Robotics Research*, vol. 35, no. 12, pp. 1497–1521, 2016.

[21] S. Rezazadeh and J. W. Hurst, "Toward step-by-step synthesis of stable gaits for underactuated compliant legged robots," in *2015 IEEE International Conference on Robotics and Automation (ICRA)*. IEEE, 2015, pp. 4532–4538.

[22] A. Hereid, M. J. Powell, and A. D. Ames, "Embedding of slip dynamics on underactuated bipedal robots through multi-objective quadratic program based control," in *53rd IEEE Conference on Decision and Control*. IEEE, 2014, pp. 2950–2957.

[23] S. Rezazadeh, C. Hubicki, M. Jones, A. Peekema, J. Van Why, A. Abate, and J. Hurst, "Spring-mass walking with atrias in 3d: Robust gait control spanning zero to 4.3 kph on a heavily underactuated bipedal robot," in *ASME 2015 dynamic systems and control conference*. American Society of Mechanical Engineers Digital Collection, 2015.

[24] J. R. Dormand and P. J. Prince, "A family of embedded runge-kutta formulae," *Journal of computational and applied mathematics*, vol. 6, no. 1, pp. 19–26, 1980.

[25] A. De Luca, A. Albu-Schaffer, S. Haddadin, and G. Hirzinger, "Collision detection and safe reaction with the dlr-iii lightweight manipulator arm," in *2006 IEEE/RSJ International Conference on Intelligent Robots and Systems*. IEEE, 2006, pp. 1623–1630.

[26] M. H. Raibert, H. B. Brown Jr, and M. Chepponis, "Experiments in balance with a 3d one-legged hopping machine," *The International Journal of Robotics Research*, vol. 3, no. 2, pp. 75–92, 1984.

[27] J. Pratt, J. Carff, S. Drakunov, and A. Goswami, "Capture point: A step toward humanoid push recovery," in *2006 6th IEEE-RAS international conference on humanoid robots*. IEEE, 2006, pp. 200–207.

[28] E. Rohmer, S. P. Singh, and M. Freese, "Coppeliasim (formerly v-rep): a versatile and scalable robot simulation framework."

[29] E. Coumans *et al.*, "Bullet physics library," *Open source: bulletphysics. org*, vol. 15, no. 49, p. 5, 2013.